© 2018. Published by The Company of Biologists Ltd | Development (2018) 145, dev159558. doi:10.1242/dev.159558

RESEARCH ARTICLE

Ma2/d promotes myonuclear positioning and association with the sarcoplasmic reticulum

Adriana Reuveny, Marina Shnayder, Dana Lorber, Shuoshuo Wang* and Talila Volk‡

ABSTRACT

The cytoplasm of striated myofibers contains a large number of membrane organelles, including sarcoplasmic reticulum (SR), T-tubules and the nuclear membrane. These organelles maintain a characteristic juxtaposition that appears to be essential for efficient inter-membranous exchange of RNA, proteins and ions. We found that the membrane-associated Muscle-specific $\alpha 2/\delta$ (Ma2/d) subunit of the Ca^{2+} channel complex localizes to the SR and T-tubules, and accumulates at the myonuclear surfaces. Furthermore, *Ma2/d* mutant larval muscles exhibit nuclear positioning defects, disruption of the nuclear-SR juxtapositioning, as well as impaired larval locomotion. Ma2/d localization at the nuclear membrane depends on the proper function of the nesprin ortholog Msp300 and the BAR domain protein Amphiphysin (Amph). Importantly, live imaging of muscle contraction in intact *Drosophila* larvae indicated altered distribution of Sarco/Endoplamic Reticulum Ca^{2+}-ATPase (SERCA) around the myonuclei of *Ma2/d* mutant larvae. Co-immunoprecipitation analysis supports association between Ma2/d and Amph, and indirectly with Msp300. We therefore suggest that Ma2/d, in association with Msp300 and Amph, mediates interactions between the SR and the nuclear membrane.

KEY WORDS: Amphiphysin, Ca^{2+} channel, Nesprin, Muscle, Sarcoplasmic reticulum, *Drosophila*

INTRODUCTION

Fully differentiated skeletal muscle fibers are multinucleated, elongated cells with highly ordered cytoplasm, essential for efficient muscle contraction and organismal movement. Muscle nuclei are positioned evenly along the contractile axis, and are typically located between the myofilament compartment and the plasma membrane, in close proximity to T-tubule membrane indentations, and the sarcoplasmic reticulum (SR) (Cadot et al., 2015; Folker and Baylies, 2013; Gundersen and Worman, 2013). Despite significant cytoplasmic flow produced by muscle contractile/relaxation waves, the relative position of myonuclei, T-tubules and SR remains robust in mature muscle fibers, implicating certain connectivity between these organelles. Importantly, the maintenance of myonuclei position and shape appears to be essential for muscle function, as their abnormal aggregation is observed in a variety of muscle diseases, including Emery Dreifuss muscular dystrophy (EDMD) (Muchir and Worman, 2007; Puckelwartz and McNally, 2011; Puckelwartz et al., 2009; Zhang et al., 2007), cardiac diseases, centronuclear myopathy (CNM) (Jungbluth and Gautel, 2014) and others. The mechanisms controlling myonuclear position relative to the SR are largely unknown.

Recent studies in model organisms, including *Drosophila*, zebrafish, *C. elegans* and mice, have identified a number of molecular components required for nuclear positioning in muscle fibers. These include nesprins (Elhanany-Tamir et al., 2012; Fischer et al., 2004; Starr and Han, 2002; Technau and Roth, 2008; Volk, 1992), SUN-domain proteins (Cain et al., 2014; Kracklauer et al., 2007; McGee et al., 2006), lamins (Bank et al., 2011; Dialynas et al., 2012; Dialynas et al., 2010; Mattout et al., 2011), Amphiphysin (D'Alessandro et al., 2015; Mathew et al., 2003; Razzaq et al., 2001) and Myotubularin (Ribeiro et al., 2011; Yu et al., 2012), and the microtubule-binding proteins Map7 (also known as Esconsin) (Metzger et al., 2012), Kinesin (Folker et al., 2014), Dynein (Folker et al., 2012; Schulman et al., 2014), ACF7/Shot (Wang et al., 2015) and EB1 (Wang et al., 2015). Whereas proteins such as Esconsin, Kinesin, Dynein and Klar (a *Drosophila* nesprin-like protein), and Klaroid (a *Drosophila* SUN domain protein) appear to mediate nuclear transport during myotube development, contributing to the initial nuclear position, others, including Msp300, Amphyphisin, lamins, Myotubularin, Shot (a *Drosophila* ACF7-like protein) and EB1, are required in fully differentiated muscle fibers (Volk, 2012). Hence, their function correlates with the establishment of the sarcomere structures and the onset of muscle contraction. Although the functional data regarding these gene products has been obtained primarily from model organisms, the structural similarity with their mammalian orthologs is expected to uncover basic mechanisms that regulate organelle positioning within striated contractile muscle fibers.

Msp300, the *Drosophila* ortholog of mammalian nesprin 1 (SYNE1) and nesprin 2 (SYNE2), produces isoforms with a KASH domain (a domain inserted into the outer myonuclear membrane) and isoforms lacking the KASH domain, which localize at distinct cytoplasmic domains, including along the perinuclear microtubule, Z-discs and post-synaptic buttons (Elhanany-Tamir et al., 2012; Morel et al., 2014; Packard et al., 2015). Msp300 labeling is often observed as thin filaments with elastic properties, which link the nucleus with Z-discs, and postsynaptic buttons. In *Msp300* homozygous mutant larvae, the myonuclei aggregate and dissociate from the perinuclear microtubule network, leading to defective muscle function (Elhanany-Tamir et al., 2012). Amphiphysin (also known as BIN1) (Amph), a N-terminal bar-domain protein with a C-terminal SH3 motif, is required for membrane curvature during endocytosis and recycling, as well as for T-tubule biogenesis in *Drosophila* muscles (Lee et al., 2002; Mathew et al., 2003; Razzaq et al., 2001; Royer et al., 2013). Recent findings indicated that, in cultured differentiating myotubes and in *C. elegans* epithelial seam cells, Amph is required for nuclear

Department of Molecular Genetics, Weizmann Institute, Rehovot 76100, Israel. *Present address: Institute of Systems Genetics, New York University School of Medicine, NYU Langone Health, New York, NY 10016, USA.

‡Author for correspondence (talila.volk@weizmann.ac.il)

T.V., 0000-0002-3800-2621

Received 18 September 2017; Accepted 24 July 2018

Development (2018) 145, dev159558. doi:10.1242/dev.159558

positioning (Adam et al., 2015; Caldwell et al., 2014; D'Alessandro et al., 2015; Falcone et al., 2014). Amph interactions with N-WASP and ANC-1 (the *C. elegans* nesprin 1 ortholog), as well as with CLIP 170, have been shown to be important for myonuclear positioning.

Using *Drosophila* larval muscles to uncover molecular processes promoting nuclear positioning in muscle fibers, we identified Ma2/d. The *Ma2/d* gene (also known as CG42817) is a member of a family of three genes in *Drosophila*, along with *straight jacket* (*stj*) (Ly et al., 2008; Neely et al., 2010; Tian et al., 2015) and *CG4587*, and four genes in mammals, all of which share a trans-membrane or GPI-linked domain, and a von Willebrand factor A (VWA) domain with Ca^{2+}-binding motif (Dolphin, 2012; Dolphin, 2013). Previous studies demonstrated that alpha2/delta proteins form part of the voltage-gated Ca^{2+} channel complex, which allows Ca^{2+} entry into the cell during membrane depolarization. The alpha2/delta proteins function as auxiliary components to modulate the extent of Ca^{2+} signaling in different tissues (Dolphin, 2012). In both vertebrates and invertebrates, the alpha2/delta subunit physically interacts with the Ca^{2+} channel core proteins $C\alpha_V1$ or $C\alpha_V2$ and regulates their levels at the plasma membrane, thereby indirectly controlling the extent of Ca^{2+} signaling (D'Arco et al., 2015). Clearly, the alpha2/delta subunit has additional Ca^{2+} channel-independent roles in various cell types, including muscles. In *Drosophila*, it is associated with endosomes, autophagosomes and lysosomal fusion (Tian et al., 2015). In vertebrates, alpha2/delta proteins are involved in the development and migration of myotubes independently of their role in the muscle Ca^{2+} channel complex (García et al., 2008), and in addition they couple between T-tubules and the SR (Block et al., 1988). In neurons, alpha2/delta promotes synapse formation in response to Thrombospondin or to Gabapentin, an analgesic component (Eroglu et al., 2009). Because Thrombospondin is essential for proper muscle development, both in *Drosophila* and zebrafish (Subramanian and Schilling, 2014; Subramanian et al., 2007), we investigated the role of alpha2/delta in *Drosophila* muscle development.

Our results imply that Ma2/d contributes predominantly to nuclear association with the SR, as well as to nuclear positioning in striated muscles. Ma2/d localizes along the T-tubules and SR, and accumulates along the nuclear membrane. Larval muscles lacking functional Ma2/d exhibit abnormal myonuclear position, disruption of nuclear-SR juxtaposition and slower locomotive activity.

RESULTS

Ma2/d is localized along the T-tubules and SR, and at the nuclear membrane

To reveal the subcellular distribution of Ma2/d in muscle fibers, we produced flies expressing Ma2/d-GFP by fusing full-length Ma2/d with GFP at its most C-terminal sequence (Fig. 1, upper panel), and expressed it using a muscle-specific Mef2-GAL4 driver. Importantly, this overexpression did not affect normal development and flies expressing Ma2/d-GFP were viable. Co-labeling of GFP with Amphiphysin (Amph) indicated numerous sites of elongated structures labeled with Ma2/d-GFP and decorated with punctate Amph, corresponding to T-tubules (Fig. 1A-A″, empty arrows). In addition, Amph-positive dots around the nuclear membrane often overlapped Ma2/d-GFP (Fig. 1A-A‴, arrows). Furthermore, Ma2/d-GFP labeling surrounded each of the myonuclei, and corresponded to the SR, as indicated by overlap labeling with SERCA (Fig. 1C-C″). To discriminate between plasma membrane versus SR membranes, larvae were labeled with a recently described plasma membrane fluorescent dye, 'membrane-binding fluorophore-cysteine-lysine-palmitoyl' (mCLING), prior to fixation (Revelo and Rizzoli, 2016), and then fixed and labeled with GFP. mCLING is expected to label the plasma membrane, including T-tubules surfaces, but not the SR membrane. Consistent with localization of Ma2/d-GFP in the SR, we detected GFP labeling surrounding the myonuclei that was mCLING-negative (Fig. 1B-B″, empty arrows). In addition, Ma2/d-GFP labeled structures that were closely related to mCLING and accumulated at the myonuclear periphery, presumably labeling points of intersection between T-tubules and the SR or nuclear membrane (Fig. 1B-B‴, filled arrows). Co-labeling of anti-GFP with SERCA revealed overlap localization around the myonuclei (Fig. 1C-C″, filled arrows), as well as along the T-tubule-associated SR (Fig. 1C-C″, empty arrows). It was concluded that Ma2/d-GFP distribution was confined to the SR, T-tubules and to Amph-positive nuclear associated dots. Although the Ma2/d-GFP was overexpressed by Mef2-GAL4 and might not represent endogenous levels, the overexpression did not affect viability of the larvae and flies, nor did it affect larval locomotion (data not shown).

To confirm the distribution of Ma2/d in muscles, an antibody raised against a mixture of three conserved peptides (each fused to KLH) of the Ma2/d extracellular domain was produced (the epitopes and peptides are indicated in Fig. 2, upper panel). Specificity of the antibody was verified by its positive reactivity with ectopically expressed Ma2/d-GFP in the wing imaginal disc (Fig. S1A-C) and by western blot (Fig. S1D,E). The anti-Ma2/d antibody exhibited overlapping distribution with the muscle-driven Ma2/d-GFP (Fig. 2A-A″), confirming its distribution at the T-tubules, SR and nuclear periphery. Furthermore, the anti-Ma2/d antibody exhibited overlapped distribution with SERCA at the perinuclear region, confirming their colocalization at this region (Fig. 2B-B″). Collectively, it was concluded that Ma2/d localizes to T-tubules, SR and the nuclear periphery.

Production of Ma2/d mutant larvae

We performed knockout of the *Ma2/d* gene by a P-element excision of a transgene insertion $EPgy2^{EY2EY09750}$ located at the first intron of the gene. Sequence analysis of the genomic region following the P element excision indicated a deletion and rearrangement within the first intron, 5′ to the P element, extending to the end of the first exon, presumably interfering with its proper splicing (Fig. S2). Because an additional methionine residing in the third exon might provide a translation start site, the mutant larvae were expected to express a truncated Ma2/d protein of ∼80 kDa, which should still be recognized by the antibody; however, such a protein is not expected to be functional owing to the lack of a signal peptide. Adult flies mutant for this allele were homozygous lethal and, in addition, were lethal in trans over a chromosomal deficiency [Df(2L)BSC293] that removed the corresponding genomic region, confirming that lethality is due to *Ma2/d* destruction. The homozygous mutant larvae carrying the heteroallelic combination of *Ma2/d /Df(2L)BSC293* were further analyzed to reveal the contribution of *Ma2/d* to the proper development of the somatic musculature.

Western analysis with the anti-Ma2/d antibody recognized a specific band in the protein extract of larvae expressing the Ma2/d-GFP (driven by muscle-specific Mef2-GAL4) of the expected 170 kDa size (140 kDa of full-length Ma2/delta fused to GFP), and this band was also reactive with anti-GFP antibody (Fig. S1E, left panel), confirming antibody specificity. The anti-GFP also recognized a 50 kDa band by western analysis, representing the cleaved delta subunit fused to GFP (Fig. S1E, left panel). This band was not reactive with the anti-Ma2/d antibody, as it was raised

Development (2018) 145, dev159558. doi:10.1242/dev.159558

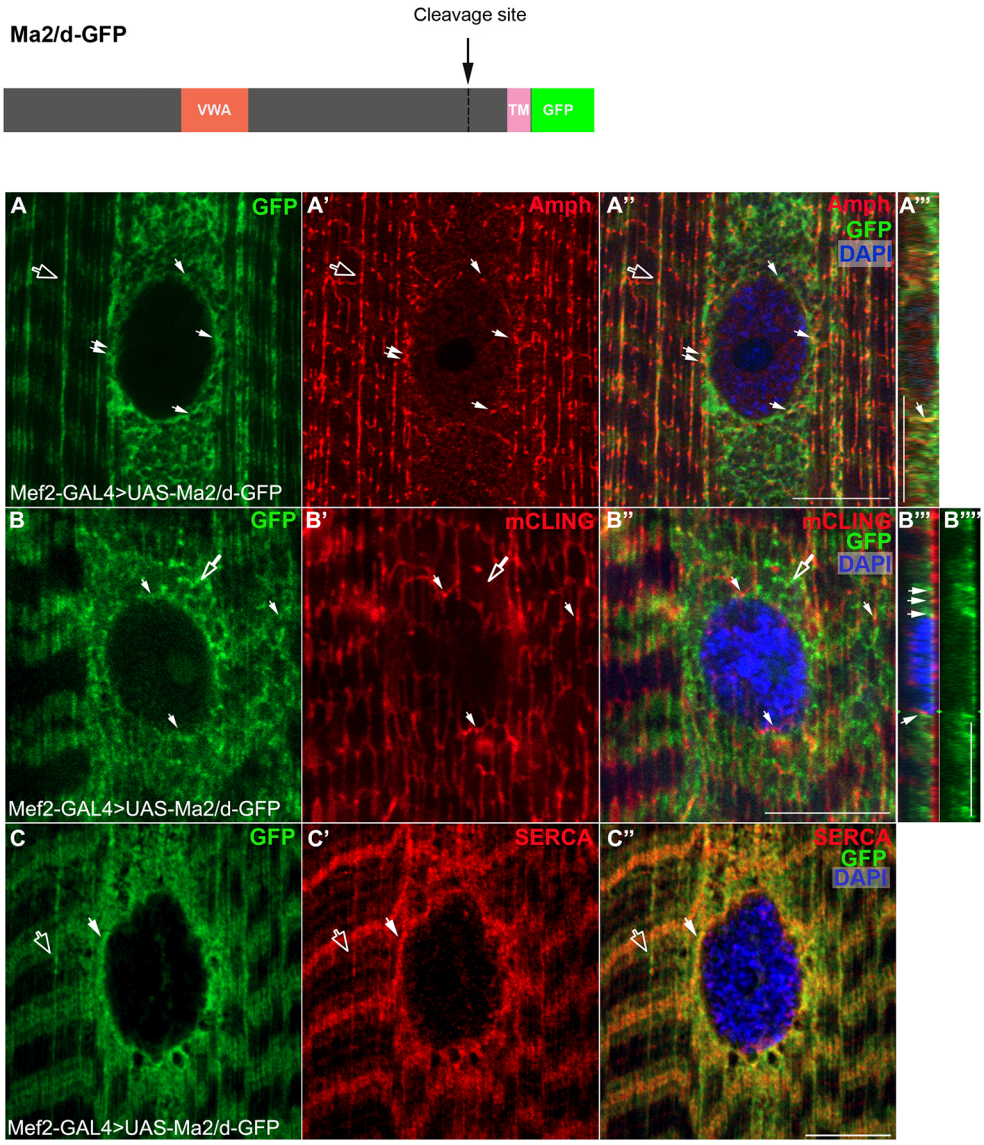

Fig. 1. Ma2/δ-GFP localization in myofibers corresponds to SR and T-tubules. Top: domain structure of Ma2/d-GFP. (A-C″) Single confocal images of flat preparations of 3rd instar larval muscles expressing Ma2/d-GFP and labeled using anti-GFP antibodies (green, A,A″,A‴,B,B″,B‴,B⁗,C,C″) and using anti-Amphiphysin (red, A′-A‴), mCLING (red, B′-B‴) or anti-SERCA (red, C′,C″) antibodies. A‴ and B‴ and B⁗ are orthogonal sections of the nuclei shown in A″ and B″, respectively. White arrows in A-A‴ indicate sites along the myonuclei where Ma2/d-GFP and Amphiphysin colocalize. Empty arrows in A-A‴ indicate longitudinal T-tubules. White arrows in B-B⁗ indicate sites where Ma2/d-GFP and mCLING are proximal. Empty arrows in B-B″ indicate sites of negative overlap. White arrows in C-C″ indicate sites of colocalization of Ma2/d-GFP and SERCA at the nuclear-associated SR; empty arrows indicate sites of colocalization of Ma2/d-GFP and SERCA at the T-tubules. A-C show a single optical confocal stack. Scale bars: 10 µm.

against sequences located N-terminal to the cleavage site (Fig. S1D). Importantly, whereas the anti-Ma2/d recognized a protein band of 140 kDa in a protein extract of wild-type larvae it reacted with a protein band of ∼80 kDa in *Ma2/d* mutant larvae (Fig. S1, right panel). This band apparently represents the truncated Ma2/d mutant protein. Furthermore, staining of the *Ma2/d* mutant larvae with anti-Ma2/d did not show specific staining (Fig. 2C,D), implying that the truncated protein observed by the western blot was not localized properly, possibly because it lacks the signal peptide. We concluded that the hetero-allelic combination of EPgy2Δ^{EY2EY09750}/Df(2L)BSC293 mutant larvae lack functional Ma2/d and therefore further analyzed the phenotype of larvae carrying this allelic combination (refers to *Ma2/d* in all figures).

Ma2/d mutant muscles exhibit abnormal nuclear position

The muscles of the *Ma2/d* mutant larvae exhibited abnormal nuclear positioning phenotype where the myonuclei were significantly closer to each other and often created small aggregates (Fig. 3A-B‴, C, and see Fig. S3 indicating aberrant myonuclear position following knockdown of *Ma2/d* with RNAi driven by Mef2-GAL4 driver). Of note, the *M2/d* mutant muscle length remained unchanged (Fig. S3). This phenotype was reminiscent of that observed in the LINC complex mutants *Msp300*, *klar* and *koi*, although it was less severe (Elhanany-Tamir et al., 2012). Interestingly, the typical perinuclear distribution of Msp300, which normally forms a ring surrounding each myonucleus, was altered and the protein often aggregated in the vicinity of the nucleus (Fig. 3A,B, arrow). In contrast, Msp300 localization appears normal at the Z-bands. We therefore concluded that Ma2/d is required for promoting Msp300 nuclear localization as well as for proper myonuclear positioning.

To reveal the physiological requirement for Ma2/d, we performed a larval locomotion assay for the mutant larvae as previously described (Elhanany-Tamir et al., 2012). The *Ma2/d* mutant larvae were 41% slower relative to wild-type larvae (Fig. 3D; $P<0.005$; $n=7$), implying an important contribution of Ma2/d for muscle function.

Ma2/d mutant muscles exhibit defects in the nuclear-SR association

Further analysis indicated that SERCA, which marks both the SR along the T-tubules and the SR associated with the myonuclei, is

Development (2018) 145, dev159558. doi:10.1242/dev.159558

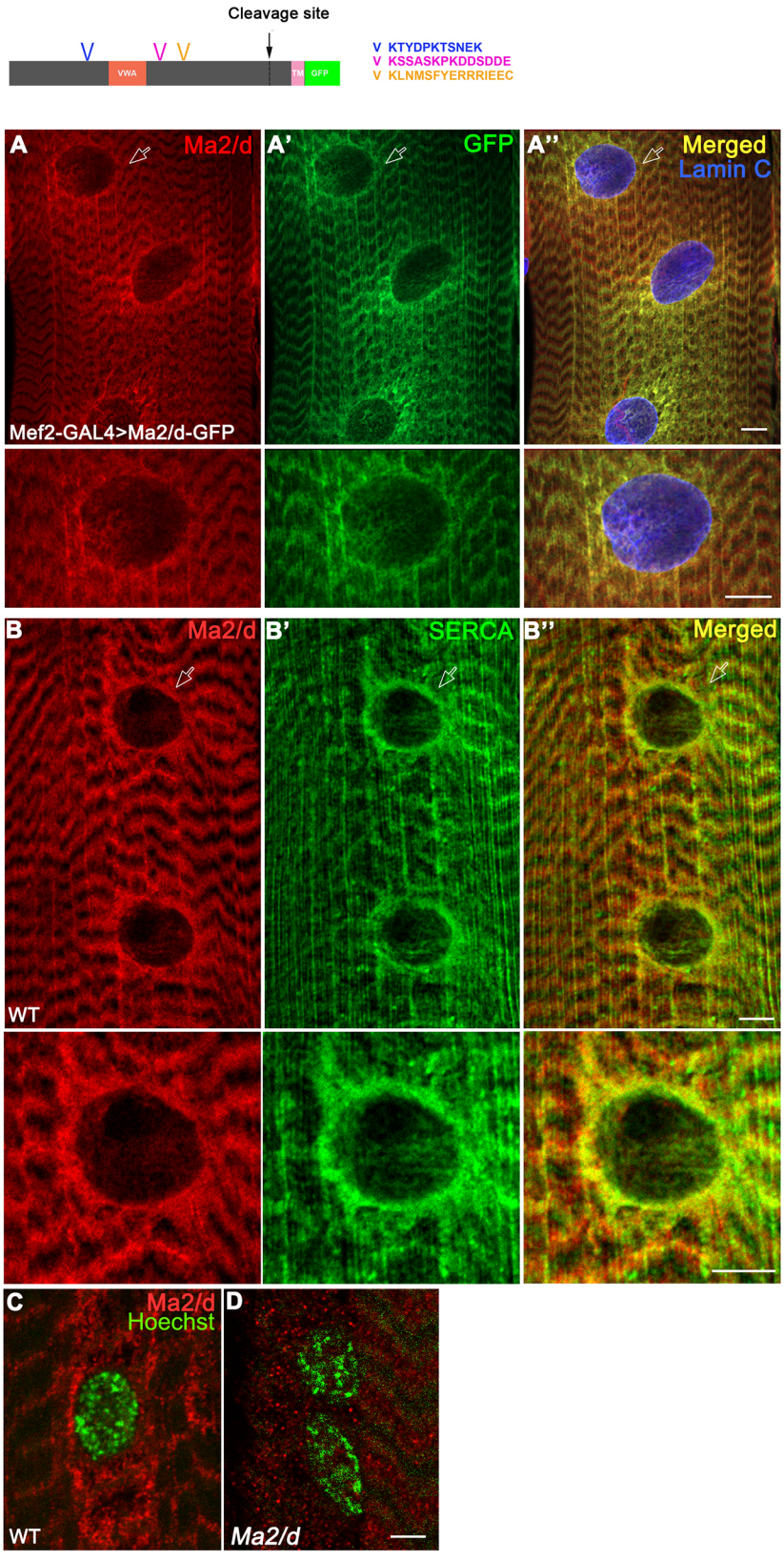

Fig. 2. Ma2/d antibody reactivity in wild-type and *Ma2/d* mutant muscles. Top: three peptides used for production of the anti-Ma2/d protein. (A-A″) Single confocal stacks of larval muscles expressing Ma2/d-GFP labeled using anti-Ma2/d antibody (A, red) and anti-GFP antibody (A′, green). The nuclei are labeled with Lamin C (A″, blue). Enlarged images of single nuclei (marked by arrows) are shown in the lower panels, indicating a high degree of overlap between the anti-Ma2/d and Ma2/d-GFP. (B-B″) Single confocal stack of larval muscle labeled using anti-Ma2/d (red) and anti-SERCA (green) antibodies, and their merged image (B″). The nucleus indicated by arrows is enlarged in the corresponding lower panels. There is an intense labeling for Ma2/d at the perinuclear region, which overlap with SERCA. (C,D) 3rd instar larval muscles stained using anti-Ma2/d (red) in wild-type (C) or in *Ma2/d* mutant (D) muscles. The antibody does not react with muscles of the mutant larvae. Hoechst labels the muscle nuclei (green). Scale bars: 10 µm.

significantly reduced in the vicinity of the perinuclear membrane, and its distribution is abnormal, forming small aggregates in the muscles of *Ma2/d* mutant larvae (Fig. 4A-B′). We quantified SERCA peak fluorescence intensity at the nuclear periphery relative to background levels at the nuclear interior along the nuclear meridian (see example in Fig. 4D). A significant reduction in SERCA levels at the nuclear periphery (normalized to background levels) was observed in *Ma2/d* mutant myonuclei relative to control (Fig. 4E; *t*-test $P=9\times10^{-18}$; the wild-type group included $n=40$ nuclei, measured from three larvae, in 10 different number 6

Development (2018) 145, dev159558. doi:10.1242/dev.159558

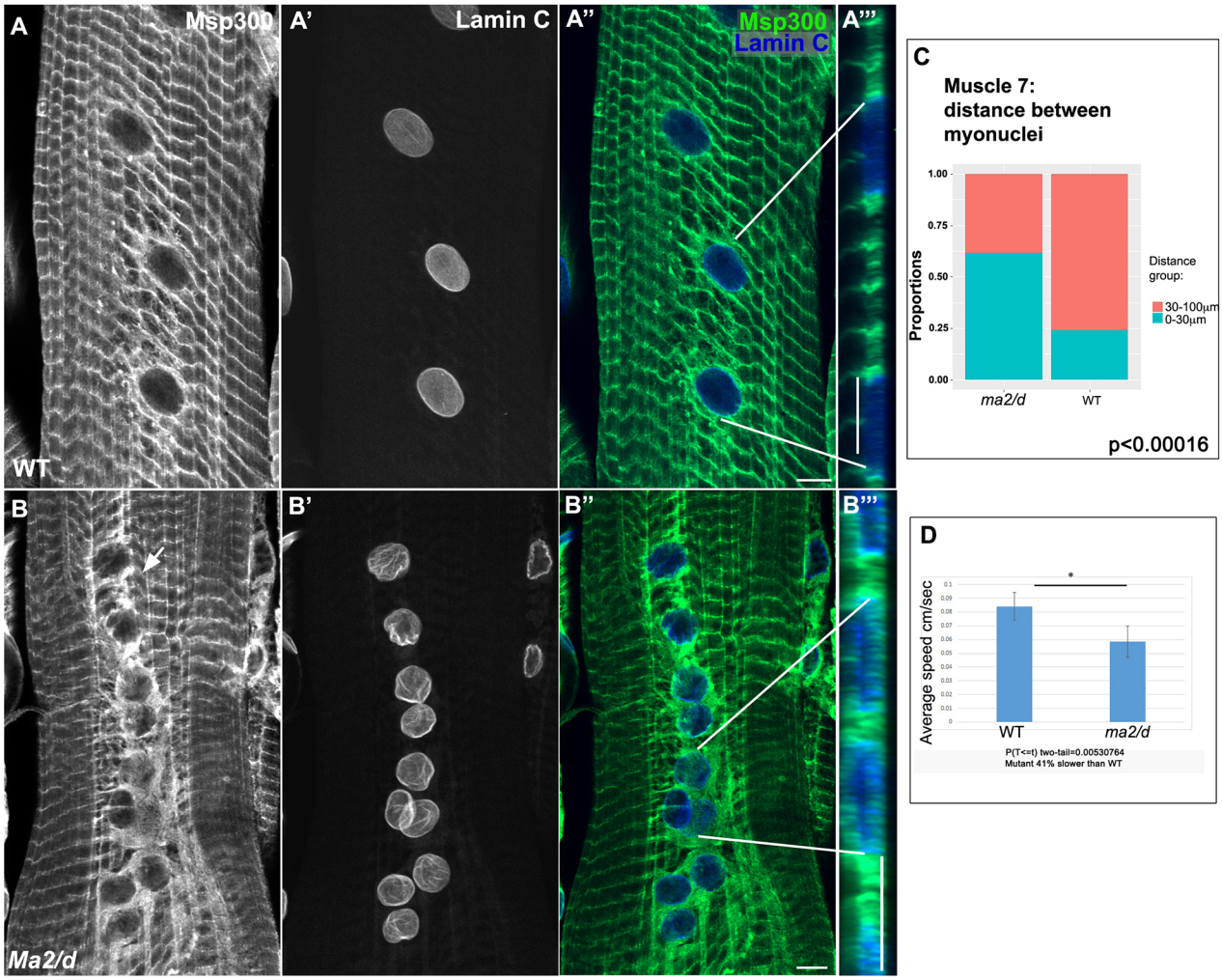

Fig. 3. Ma2/d is required for nuclear positioning and proper Msp300 nuclear localization. Single confocal stacks of muscles from wild-type (A-A‴) and *Ma2/d* mutant (B-B‴) labeled using anti-Msp300 (green A″,A‴,B″,B‴) and anti-lamin C (white in A,A′,B,B′ and blue in A″,A‴,B″,B‴) antibodies. Note the aberrant nuclear position in *Ma2/d* mutant muscles, and Msp300 accumulation around the nuclei. Orthogonal sections (A‴,B‴) indicate the accumulation of Msp300 above and around the myonuclei in mutant muscles. (C) Quantification of the distances between nuclei of muscle six in wild type and the *Ma2/d* mutant. In the wild-type muscle, most of the nuclei were at a comparable distance of 30-100 µm from each other (76.4%), whereas in *Ma2/d* mutant muscle, most of the nuclei were closer to each other and only 37.4% were at a distance similar to wild type (P<0.00016). (D) Quantification of the locomotion of wild-type and *Ma2/d* mutant larvae. n=7, *P<0.005. Scale bars: 10 µm.

muscles; the mutant group included n=29 nuclei analyzed from three larvae, from eight different number 6 muscles). Importantly, a concomitant measurement of Lamin C fluorescence peaks at the nuclear membrane (normalized to background levels) in the same optical section, indicated that Lamin C levels did not change significantly in the *Ma2/d* mutant myonuclei, relative to control (Fig. 4F; t-test P=0.3; same nuclei as above). The reduced perinuclear distribution of SERCA was also observed when we knocked down *Ma2/d* in muscles following muscle-specific expression of *Ma2/d* RNAi (Fig. S3). Importantly, the reduced SERCA levels at the nuclear periphery were partially rescued by a muscle-specific expression of Ma2/d-GFP in the mutant *Ma2/d* larvae (Fig. 4C,C′,D,E; t-test P=0.001; the rescue group included n=37 nuclei, analyzed from 10 muscles from five distinct larvae; the mutant group was as above). Lamin C levels did not change significantly between the mutant and rescue groups (t-test P=0.1). Of note, overexpression of Ma2/d in the mutant *Ma2/d* muscles did not rescue SERCA levels to the extent of control muscles, possibly indicating that it is not fully active (comparison between SERCA levels in the rescue nuclei versus control indicates a significant difference, t-test $P=3\times10^{-10}$; the number of nuclei of the rescue and control groups are indicated above). Lamin C levels were comparable between the rescue and control groups (t-test P=0.2). We therefore concluded that Ma2/d is required for proper SERCA distribution in the vicinity of the nuclear membrane.

To further address the contribution of Ma2/d to SR-nucleus association in intact larvae, during muscle contraction we imaged immobilized live intact larvae expressing either Ma2/d GFP or SERCA-Cherry in control muscles or in *Ma2/d* mutant larvae, and followed their distribution during muscle contractile waves. This was performed by immobilization of live larvae expressing muscle-specific Ma2/d-GFP or Cherry-SERCA and their imaging under the spinning disc microscope (Fig. 5). We detected two Ma2/d-GFP-positive perinuclear structures: a tight nuclear ring (Fig. 5A, empty arrowhead) and an outer wider ring (Fig. 5A, empty arrow) that is continuous with the transverse SR along the T-tubules (Fig. 5A, filled arrow). Notably, thin M2/d-GFP positive threads extend between the two perinuclear rings (Fig. 5A′, white filled arrow).

Development (2018) 145, dev159558. doi:10.1242/dev.159558

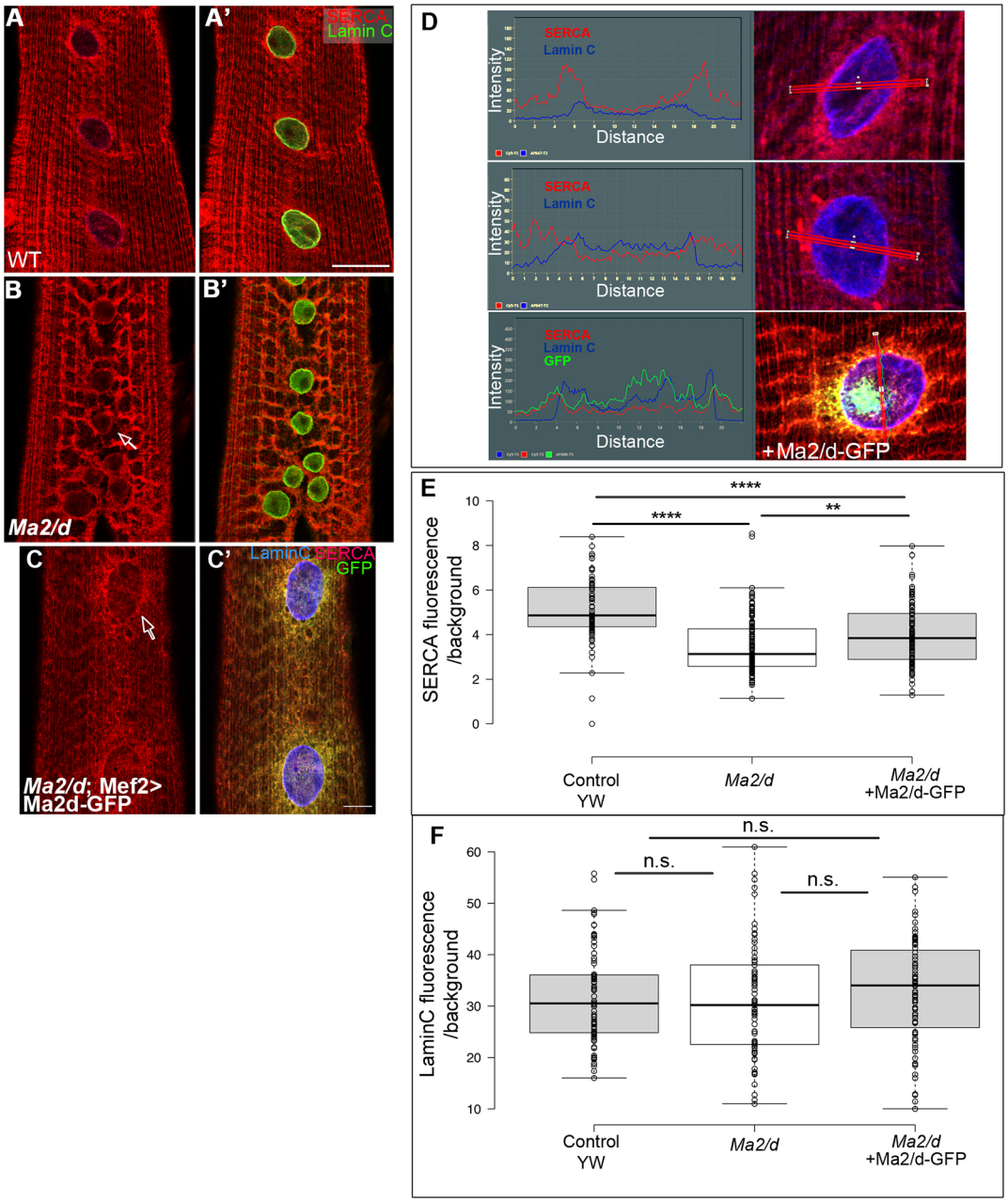

Fig. 4. Decreased distribution of perinuclear SERCA in *Ma2/d* mutant muscles. Single confocal stacks of wild-type (A,A′) or *Ma2/d* mutant (B,B′) muscles labeled using anti-SERCA (red, A-B′) and anti-Lamin C (green, A′,B′) antibodies. SERCA distribution is often reduced at the nuclear membrane (arrow in B). (C,C′) Representative images of a rescue experiment demonstrating single confocal stacks of larval muscle in which Ma2/d-GFP driven by the Mef2-GAL4 driver was expressed in a *Ma2/d* mutant larva (red, SERCA). (C′) Merged images of SERCA (red), Ma2/d-GFP (green) and Lam C (blue). (D-F) Quantification of SERCA and Lamin C at the perinuclear region. (D) Representative examples of the quantification method in which the fluorescent profile is taken from SERCA (red) or from Lamin C (blue) in wild type (top panel) or *Ma2/d* mutant (middle panel). The red rectangular box indicates the meridian axis. Bottom panel shows an example of the fluorescent profile of the rescue experiment. (E) Quantification of peak SERCA fluorescence intensity/background (SERCA at the nuclear envelope normalized to SERCA in the center of the nucleus) along the nuclear meridian in control (YW), *Ma2/d* mutant and in *Ma2/d* rescued with Ma2/d-GFP muscles, indicating a significant difference between the first two groups (*t*-test, ****P=9E-18; for wild type, n=40 nuclei from 10 different muscles from three distinct larvae were quantified; for *Ma2/d*, n=29 nuclei from eight different muscles from three distinct larvae were quantified; the rescue group included n=37 nuclei, analyzed from 10 muscles from five distinct larvae). SERCA levels in the rescue group did not reach the levels of control and there was a significant difference between the two groups (*t*-test, **P=2.9E-10), indicating only partial rescue. (F) Quantification of the corresponding Lamin C peak fluorescent/background (measured at the same focal plane as SERCA) in each of the experimental groups. No significant difference in Lamin C levels between the control (YW) and *Ma2/d* mutant muscles was observed (*t*-test, P=0.3). Similarly, no significant difference in Lamin C levels between the rescue group and the control was observed (*t*-test, P=0.2). No significant difference between the rescue group and the mutant group were observed (*t*-test, P=0.1). Numbers of nuclei are the same as for SERCA. Scale bars: 10 µm.

These threads possibly represent membrane extensions connecting the distinct SR compartments. Importantly, during the contractile wave (Fig. 5A″,A‴), the two nuclear rings move together with the transverse SR-associated T-tubules (Fig. 5A, white arrow) and the thin membrane connections, implying their physical connectivity (see also Movie 1). We therefore concluded that

Development (2018) 145, dev159558. doi:10.1242/dev.159558

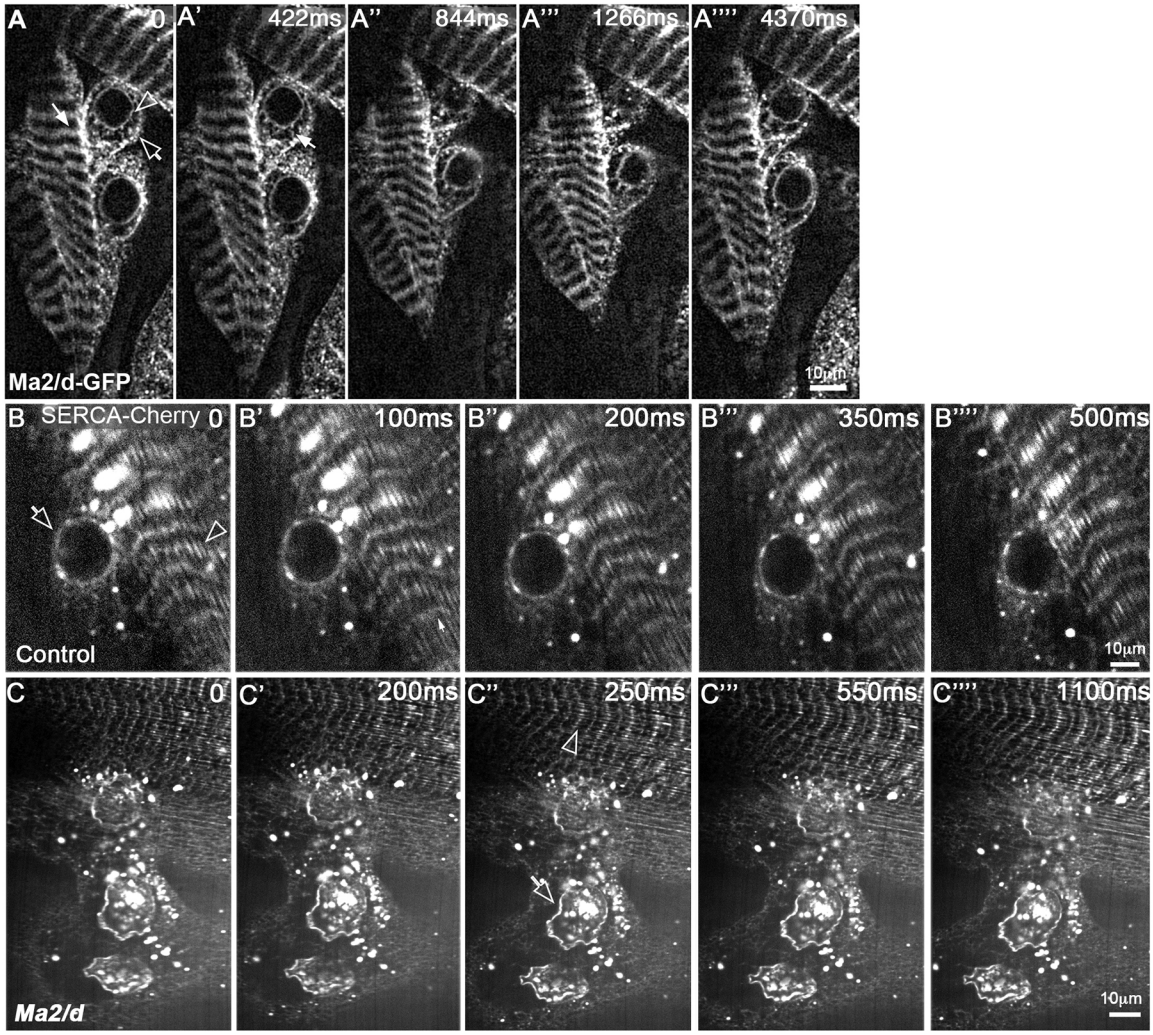

Fig. 5. Live imaging of Ma2/d-GFP and SERCA-Cherry in control and *Ma2/d* mutant larval muscles. Still images from a movie of live intact larvae expressing Ma2/d-GFP in muscles during a single contractile event. A-A‴ are images of a distinct time series. Times are indicated in each image (the entire movie is shown in Movie 1). Empty arrowhead and empty arrow in A indicate SR; the white arrow in A indicates the T-tubules. Thin GFP-positive connectors are observed between the ER and the SR surrounding the nuclei (white arrow in A′). In the course of contraction (A″,A‴), the Ma2/d-GFP-positive connections are still observed. (B,C) Still images from a movie of live intact larvae expressing SERCA-Cherry during contraction of wild-type (B-B‴) or *Ma2/d* mutant (C-C‴) larvae. Arrows in B and C″ show SERCA around the nucleus; arrowheads in B and C″ show SERCA along the T-tubules.

Ma2/d-GFP forms membrane continuity between distinct SR compartments.

Next, we expressed SERCA-mCherry in muscles of wild-type and *Ma2/d* mutant larvae, and followed its distribution in immobilized intact larval myofibers (Fig. 5B-C‴, Movies 2 and 3). Overexpression of SERCA-mCherry often forms small protein aggregates; however, the nuclear borders were clearly detected (Fig. 5B, empty arrow). SERCA-mCherry is also detected along the T-tubule-associated SR (Fig. 5B, empty arrowhead). Strikingly, in *Ma2/d* mutant muscles, the nuclear-associated SR marked by SERCA-mCherry showed irregularities at the perinuclear area during muscle contraction/relaxation (Fig. 5C,C″, arrow). We assume that these irregularities represent partial dissociation of the SR from the nuclear membrane because, after fixation, SERCA fluorescence significantly decreased at the nuclear area of *Ma2/d* mutant larvae (Fig. 4B,E). These data suggest that the association between the SR and the nucleus was partially disrupted in *Ma2/d* mutants both in fixed flat-opened larvae, as well as in intact live larvae.

Amph is required for the perinuclear distribution of Ma2/d and Msp300

Amph interactions with N-WASP, ANC-1 and CLIP 170 contribute to nuclear positioning in *C. elegans* and in differentiating myofibers in culture (D'Alessandro et al., 2015; Falcone et al., 2014). We examined the contribution of Amph to nuclear positioning, as well as to the nuclear localization of Msp300 and Ma2/d. In wild-type muscles, Msp300 and Ma2/d both colocalize around the nucleus but not along the Z-bands, where Msp300 is prominent (Fig. 6A-E′). In *Amph* mutant muscles, both Msp300 and Ma2/d dissociate from the myonuclear surfaces (Fig. 6F-J′). *Amph* mutant myonuclei showed partial or complete dissociation of Msp300 and Ma2/d from the perinuclear area in 42.9% of the myonuclei; n=46 nuclei analyzed from six muscles of three *Amph* mutant larvae. In contrast, 100% of control muscles showed normal perinuclear distribution of Ma2/d and Msp300. For Ma2/d distribution, n=76 from 15 muscles analyzed from seven larvae; for Msp300 distribution, n=65 from 12 muscles analyzed from six different larvae. This data suggests a role for Amph in connecting both Msp300 and Ma2/d to the nuclear

Development (2018) 145, dev159558. doi:10.1242/dev.159558

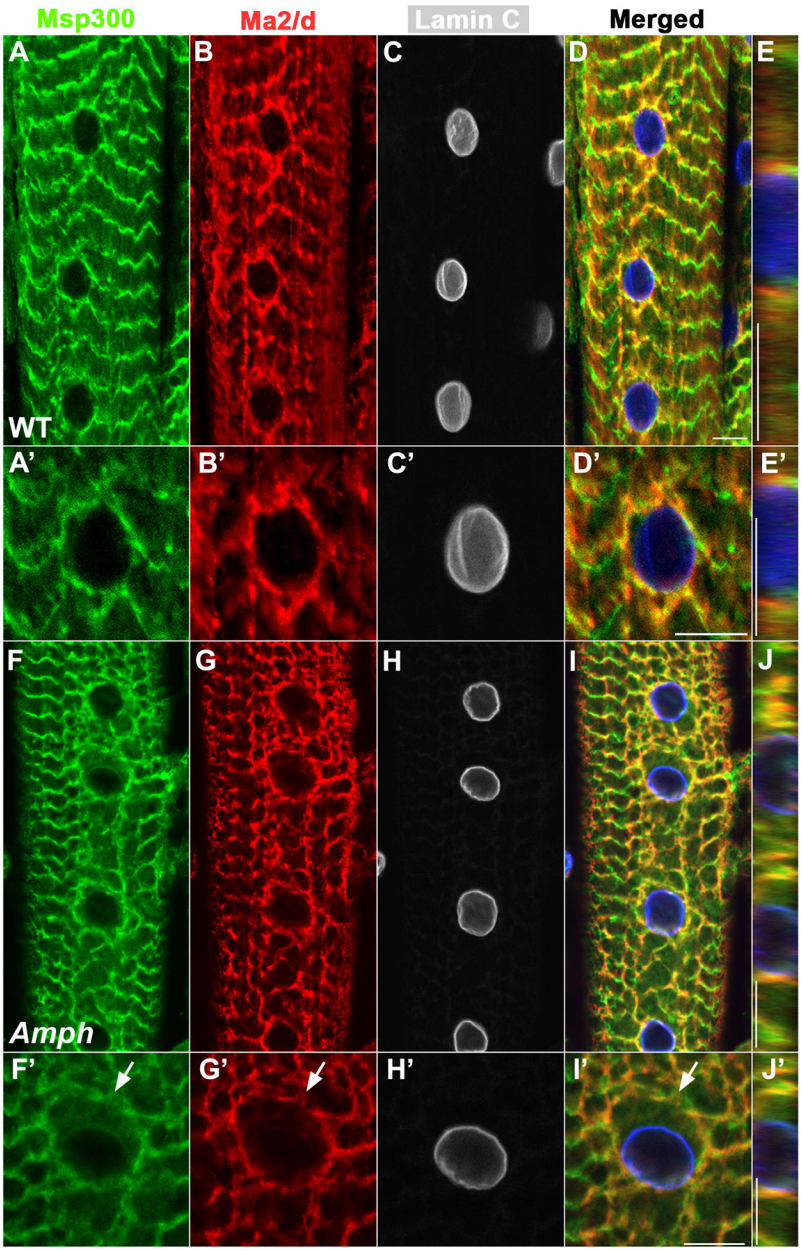

Fig. 6. Ma2/d and Msp300 distribution along the SR depends on Amphiphysin. Muscles of wild-type (A-E′) and *Amph* mutant (F-J′) of 3rd instar larvae, labeled with anti-Msp300 (green in A,A′,D,D′,E,E′,F,F′,I,I′,J,J′), anti-Ma2/d (red in B,B′,D,D′,E,E′,G,G′,I,I′,J,J′) and anti-lamin C (white in C,C′, H,H′; blue in D,D′,E,E′,I,I′,J,J′). A′-E′ and F′-J′ demonstrate corresponding enlarged images of single nuclei. In *Amph* mutants, 42.9% of the myonuclei showed partial or complete dissociation of Ma2/d and Msp300 from the perinuclear distribution (n=46) of mutant nuclei. In control, 100% of the myonuclei showed normal perinuclear distribution of Ma2/d (n=76) or Msp300 (n=65). Arrows in F′,G′,I′ indicate sites where Msp300 and Ma2/d dissociate from the myonuclei. Scale bars: 10 µm.

membrane. Despite the dissociation of Msp300 protein from the nuclear membrane in many cases, it still overlapped with Ma2/d, implicating a possible association between these proteins that is Amph independent. Consistent with previous reports, myonuclear positioning was frequently aberrant in *Amph* mutants (Fig. 6F-I′) (Razzaq et al., 2001). Abnormal SR distribution has been previously reported in *Amph* mutant muscles (Razzaq et al., 2001). Consistent with dissociation of the SR from the nuclear membrane in *Amph* mutant muscles, we detect a nuclear dissociation of Ma2/d (Fig. 6G,G′). Furthermore, the larval locomotion assay indicated that the Amph mutant larvae moved more slowly relative to control (Fig. S4).

Reciprocally, we show that, in *Msp300* mutant muscles, Amph labeling at the myonuclear area is abnormal and, furthermore, Ma2/d staining at the perinuclear area is absent (Fig. 7, compare A-C with D-F). In *Msp300* mutant nuclei, 98% showed a complete loss of Amph around the nuclear area, 81% showed complete loss of Ma2/d around the nuclear area and 18.6% showed partial loss of Ma2/d; number of mutant nuclei n=118 counted from eight muscles of four different mutant larvae. In control myonuclei, 100% showed normal perinuclear distribution of Ma2/d and Amph. For Ma2/d distribution, n=76 nuclei from 15 muscles from seven different larvae were analyzed; for Amph distribution, n=93 nuclei from 18 muscles from eight larvae were analyzed. In addition, both proteins were not distributed properly along the T-tubules (Fig. 7D). As *Msp300* mutant muscles exhibit a wide range of defects in sarcomere, mitochondria and ER exit site localization in myofibers (Elhanany-Tamir et al., 2012), it was not clear whether the abnormal distribution of Amph and Ma2/d at the nuclear periphery depended directly on Msp300.

Molecular association between Ma2/d, Amph and Msp300

To address whether Ma2/d, Msp300 and Amph form a protein complex in the larval muscles, we performed co-immunoprecipitation experiments using larvae expressing Ma2/d-GFP in muscles, and immunoprecipitated the larval protein extract with anti-GFP.

Development (2018) 145, dev159558. doi:10.1242/dev.159558

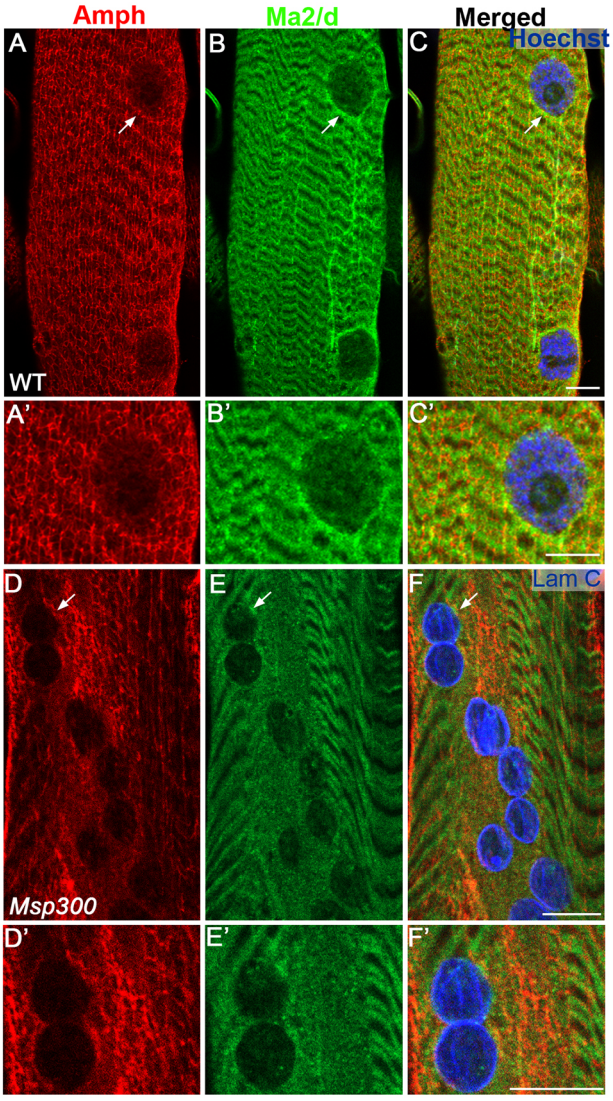

Fig. 7. Amph and Ma2/d distributions at the nuclear periphery are disrupted in *Msp300* mutant muscles. Single representative confocal stacks of larval muscles from wild-type (YW, A-C′) or Msp300$^{\Delta 3}$ mutant (D-F′) labeled with Amph (red, A,A′,D,D′) and Ma2/d (green, B,B′,E,E′), and their merged panels (C,C′,F,F′) are shown. For *Msp300* mutants, 98% of the nuclei showed complete loss of Amph and 99.6% of the nuclei showed complete or partial loss of Ma2/d (n=118 nuclei). For wild type, 100% of the nuclei showed normal perinuclear distribution for Amph (n=93) and for Ma2/d (n=76). The nuclei indicated by white arrows (A-C and D-F) are shown at higher magnification in the corresponding panels (A′-C′ and D′-F′). Scale bar: 10 µm.

Of note, these experiments were performed with muscles overexpressing Ma2/d-GFP (the levels of which might be higher relative to endogenous levels); nevertheless, it was found that Amph co-precipitated with Ma2/d-GFP in these conditions, consistent with the overlapped distribution of both proteins, and with their closely related phenotypes (Fig. 8A). We could not demonstrate co-immunoprecipitation between Ma2/d and MSP-300, possibly owing to the abundance of Msp300 in sites deficient of Ma2/d (e.g. Z-bands). In addition, Immunoprecipitation with anti-Msp300 revealed its co-precipitation with Amph (Fig. 8B), implying that these proteins form a protein complex.

Taken together, these results suggest that Amph forms a protein complex with Ma2/d, as well as with Msp-300; however, these protein complexes might be separated. Functionally, both complexes are required for nuclear positioning, as well as for perinuclear SR integrity.

DISCUSSION

Despite their large size, muscle fibers exhibit highly ordered cytoplasm in which membrane organelles, e.g. SR and mitochondria, are juxtaposed with the outer nuclear membrane (Clark et al., 2002; Gautel and Djinović-Carugo, 2016; Hong and Shaw, 2017). Nuclear juxtaposition is presumably essential for effective transport of mRNAs and proteins, as well as for efficient ion coupling across membranous compartments. How this coupling is achieved and maintained, despite the contractile nature of muscle fibers, is an important and unanswered question. Based on our experiments, we suggest that the membrane protein Ma2/d, in combination with Amphiphysin and Msp300, are essential components in maintaining SR-nuclear juxtapositioning during muscle contractile/relaxation waves.

We suggest that Ma2/d is a membrane component required for inter-membranous organelle connectivity through its association with Amph, and through the association of Amph with Msp300 (Fig. 8C). This proposed model is based on the phenotypic similarities shared between the three mutants affecting myonuclei position, and their association with the SR, as well as their overlapped distribution. Most notable is the aberrant position of the myonuclei, which correlates with both dispersed nuclear distribution of Msp300 and Amph in the *Ma2/d* mutant muscles. Additional evidence emerges from the co-immunoprecipitation data suggesting that Amph associates with Ma2/d and with Msp300.

The *Drosophila* Ma2/d protein contains a trans-membrane domain and a very short cytoplasmic tail. Our data suggest that Ma2/d forms part of a protein complex that includes Amph, a protein shown previously to promote membrane curvature, e.g. in the T-tubules (Caldwell et al., 2014; Mim and Unger, 2012; Razzaq et al., 2001). Amph could directly interact with Ma2/d cytoplasmic tail or indirectly through its association with components of the Ca^{2+} channel. We favor the second option due to the short cytoplasmic tail of Ma2/d. Although we recognize that the addition of GFP to the cytoplasmic tail of M2/d could abnormally retain a region of the Ma2/d-GFP at the SR, we do detect similar distribution of endogenous Ma2/d using the antibody raised against Ma2/d in larval muscles, supporting a correct localization of Ma2/d-GFP at these sites. At the vicinity of the nuclear membrane, we observed that Ma2/d-GFP-positive dot-like structures corresponded to extracellular mCLING-positive accumulation, which might represent points of intersection between T-tubules (labeled with mCLING at the extracellular space) and the nuclear and/or SR membranes (model in Fig. 8C). Msp300 at the nuclear membrane might provide physical support to these contact sites through its association with Amph, and with the nuclear membrane. Furthermore, dimerization of Msp300 through its multiple spectrin repeats domain, results in the formation of elongated filaments that would enhance the connections between the two organelles as described for Msp300 connections between the muscle nuclei and the neuromuscular junction (Packard et al., 2015).

The *Msp300* gene codes for multiple protein isoforms, some of them are extremely large and either contain or lack the KASH domain (Gramates et al., 2017). We have previously reported that the multiple spectrin repeats along the Msp300 sequence provide elastic properties to the connections between the nuclear membrane and the Z-discs (Wang et al., 2015). Similarly, the association between Amph and Msp300 should provide elasticity to the connections between the SR and T-tubule membranes. Taken together, our results imply that the three proteins (Ma2/d, Amph and

Development (2018) 145, dev159558. doi:10.1242/dev.159558

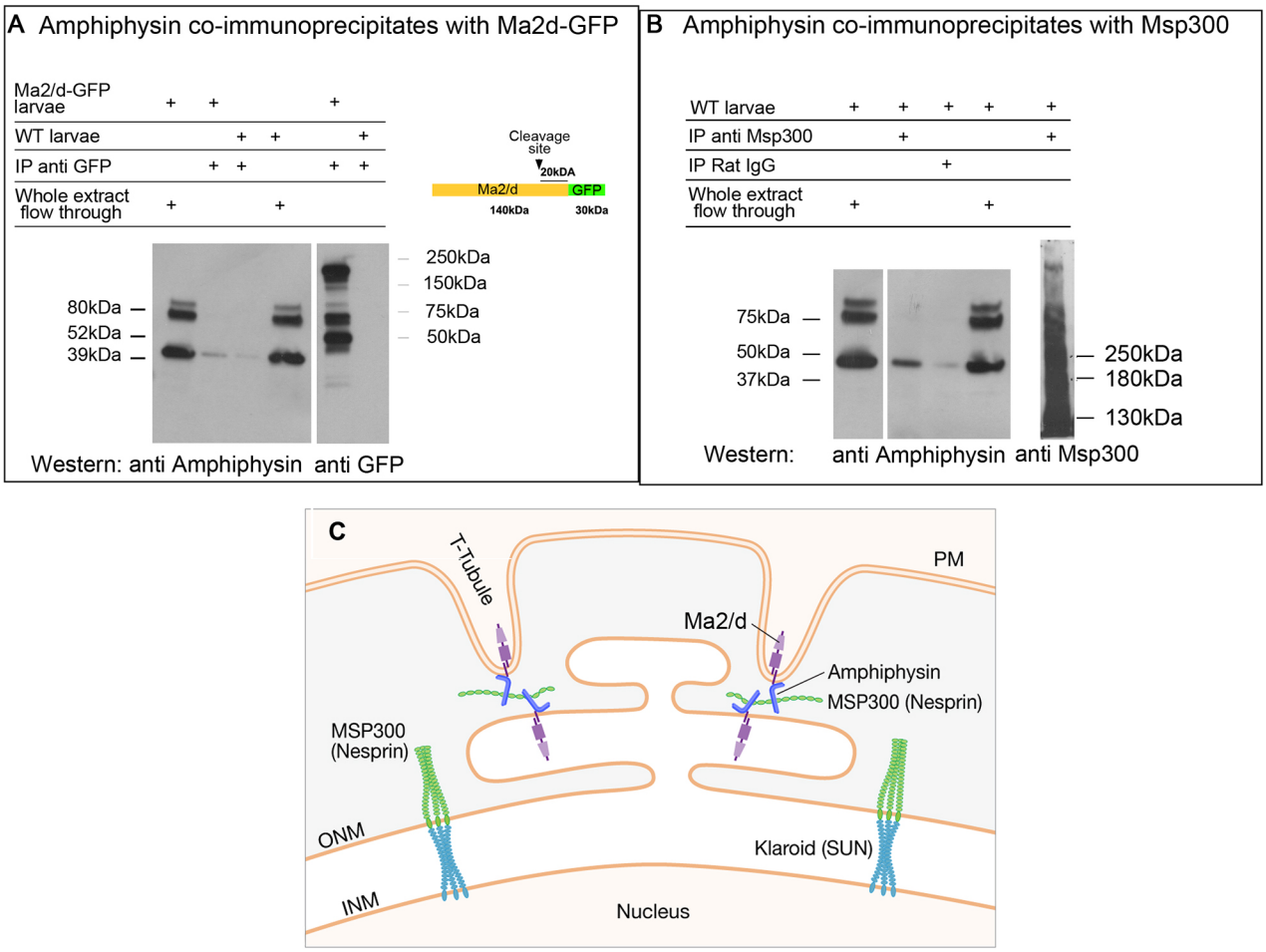

Fig. 8. Amph co-precipitates with Ma2/d and with Msp300. (A, left) Immunoprecipitation of Ma2/d-GFP expressed in larval muscles using anti-GFP antibody followed by western analysis with anti-Amph indicates a band corresponding to Amph lower band (~39 kDa), which is stronger relative to control. Whole-extract flow-through of the anti-GFP beads indicates equal loading. (A, right) GFP immunoprecipitation from control (wild type) and larvae expressing Ma2/d-GFP reacted with anti-GFP antibody indicates the 170 kDa intact Ma2/d-GFP, as well as the 120 kDa and 50 kDa cleaved forms of Ma2/d-GFP. (B, left and middle) Immunoprecipitation with anti-Msp300 antibody followed by western blotting with anti-Amph antibody indicates a smaller Amph-specific band (~39 kDa) which is stronger relative to control. Whole-extract flow-through of the anti-GFP beads indicates equal loading. (B, right) Parallel immunoprecipitation with anti-Msp300 antibody followed by a western blot with anti-Msp300 antibody, indicating several high molecular weight bands. (C) A model describing the localization and putative interactions of Ma2/d with Msp300 and with Amph. Ma2/d is present at the T-tubules and the SR membranes. It interacts with Amphiphysin at both sites. Amphiphysin interacts with a Msp300 isoform lacking the KASH domain. Interactions between these proteins mediate contact sites between the T-tubule and SR-ER membranes, which are essential for the interactions between these organelles and the myonuclei.

Msp300) mediate the formation and maintenance of contact sites between the SR and the myonuclei, presumably required to maintain SR-nuclear juxtapositioning in contractile muscles.

In vertebrates, the auxiliary subunit α2/δ protein contributes to the cell surface expression and stabilization of the $Ca_v\alpha1$ pore channel unit, and thus controls the extent of activation of the Ca^{2+} influx in neurons as well as in cardiomyocytes. This is performed by promoting $Ca_v\alpha1$ translocation from the SR compartment, as well as stabilization of the $Ca_v\alpha1$ at the plasma membrane (Canti et al., 2005; Cassidy et al., 2014; Tran-Van-Minh and Dolphin, 2010). However, it is not clear how protein translocation is promoted by α2δ. It is possible that the juxtaposition of SR to T-tubules enhances translocation of plasma membrane proteins from the SR to T-tubules in muscle fibers.

Larvae homozygous mutant for *Ma2/d* exhibited impaired locomotion. We cannot distinguish between the role of Ma2/d in regulating T-tubules/SR-nuclear contacts and its contribution to the stability of the plasma membrane $Ca_v\alpha1$ pore channel at the muscle side. We assume that both functions are necessary for proper larval locomotion. Importantly, both *Msp300* and *Amph* mutant larvae exhibit similar defective locomotion, suggesting that they both contribute to proper muscle functionality.

In conclusion, our experiments uncover novel cellular and molecular aspects that mediate membrane organelle connections in myofibers along the nuclei through the activity of *Ma2/d.* These contacts presumably contribute to an efficient transfer of mRNAs, proteins and ions between organelles, enabling proper muscle function.

MATERIALS AND METHODS

Fly stocks

Fly stocks used in this study included w^{1118} (used as a control wild type), P{GAL4-Mef2.R}, Df(2L)BSC293/CyO(YFP), Df(2L)msp300$^{\Delta3'}$/CyO(YFP), *amph*^{2j6}; P{EPgy2}CG42817 and P{TRIP.JF01922}attP2 (all of which were obtained from the Bloomington Drosophila Stock Center). *Ma2/d* mutants were obtained through imprecise excision of EPgy2^{EY09750} using a standard procedure (O'Brochta et al., 1991). The P-element excision produced rearrangement of the intronic sequences juxtaposed with the end of the first exon [see Fig. S2, according to FlyBase

Development (2018) 145, dev159558. doi:10.1242/dev.159558

(Gramates et al., 2017)]. For the rescue experiments, flies carrying either UAS-Ma2/d-GFP together with Df(2L)BSC293/CyOYFP were crossed to flies carrying excised EPgy2^{EY09750}/CyOYFP together with Mef2-GAL4/+. Mutants were identified by their negative YFP-deficient balancer.

Expression constructs

The full-length CG42817 was amplified from cDNA clone RE14947 (GenBank Accession Number BT021312, from Drosophila Genomics Resource Center), using the Gateway Cloning Technology (Invitrogen). The gene was amplified using SuperTaq Plus polymerase enzyme (Invitrogen), and inserted into the Gateway pDonor-201 vector using the following primers: attB1-FW primer, 5′-GGGGACAAGTTTGTACAAAAAAGCAGGCTTCATGTTTGGTTTATGCGAAAAG-3′; attB2-RV primer, 5′-GGGGACCACTTTGTACAAGAAAGCTGGGTCACGCATAAAGCTGTGCGTCAG-3′. The insert was then transferred to two types of destination vectors: pTWG, which contains a 5′UAS promoter, and 3′ eGFP tag (used for transgenic flies). Full-length Ma2/d-GFP was injected and transgenic flies obtained from BestGene company.

Immunochemical reagents

Primary antibody staining was performed overnight at 4°C, and the secondary staining was performed for 2 h at room temperature. We used the following primary antibodies: guinea pig anti-MSP-300 (dilution 1:300) (Volk, 1992); anti-*Drosophila* Lamin C (dilution 1:10, LC28.26) and anti-DLG 4F3 (dilution 1:50) [developed by Riemer et al. (1995) and by Parnas et al. (2001), respectively, and obtained from the Developmental Studies Hybridoma Bank]; chick anti-GFP (Abcam ab13970, dilution 1:200); rabbit anti-SERCA (obtained from Dr. Mani Ramaswami, Trinity College, Dublin, UK; dilution 1:200) (Sanyal et al., 2006); and rabbit anti-Amphiphysin (obtained from Dr. Harvey T McMahon, MRC Laboratory of Molecular Biology, Cambridge UK; dilution 1:200) (Razzaq et al., 2001). Mouse anti-GFP (Roche) was used for western blotting (dilution 1:1000) and rat anti-Ma2/d was raised against a mixture of 3 KLH-conjugated peptides from the Ma2/d sequence: peptide1, CKTYDPKTSNEKRPR; peptide2, CKSSASKPKDDSDDE (both conjugated to a KLH N-terminus domain); and peptide3, KLNMSFYERRRIEEC (conjugated to a KLH C-terminus domain) (Peptide 2.0). The resulting antibody was used at 1:500 for immunostaining and at 1:1000 for western blotting. Secondary antibodies conjugated with Cy3, Cy5 and Cy2 raised in either guinea pig, mouse or rabbit were purchased from Jackson ImmunoResearch Laboratories (dilution 1:300). Alexa Fluor 488 (Thermo Fisher Scientific) was used at 1:200 and DAPI at 1:1000 dilution (Sigma).

Fixation and immunostaining

Staining of larval flat preparations

Third instar larvae were selected and pinned on Sylgard plates (silicone elastomer-coated Petri plates, prepared by using a cocktail obtained from Dow Corning). The larvae were slit open, cleaned of fat bodies and organs, and fixed in 4% paraformaldehyde (PFA) in phosphate-buffered saline (PBS) for 25 min followed by blocking with 10% bovine serum albumin (BSA) in PBS with 0.1% Triton X-100 (PBT) for 30 min The preparations were stained overnight with primary antibody in PBT, washed with PBT, reacted with secondary antibody for 1 h, washed with PBT and mounted using Immu-Mount solution (Thermo Fisher Scientific) on a glass slide such that the somatic muscles faced the coverslip.

Immaginal disc staining

Third instar larvae expressing Ma2/d-GFP driven by the *P{GAL4}hhGal4* driver were dissected and the wing imaginal discs were fixed and stained with anti-GFP and anti-Ma2/d.

mCLING labeling and immunostaining of *Drosophila* larval flat preparations

The protocol was as described previously with minor modifications (Revelo and Rizzoli, 2016). The larvae were dissected using ice-cold physiological buffer without Ca^{2+}, cleaned of fat bodies and organs, and incubated with mCLING probe (Synaptic Systems, 710006AT1) at a concentration of 1.7 mM in physiological buffer without Ca^{2+} for 10 min at room temperature. The sample was then briefly washed with dye-free Ca^{2+}-free solution and immediately fixed in 4% PFA+0.2% glutaraldehyde in PBS for 20 min on ice followed by 20 min incubation at room temperature. The sample was then briefly washed with PBS and incubated for 5 min in quenching solution (sodium borohydride in 50 ml PBS). The sample was then briefly washed in PBS and placed in antigen-retrieval solution (R&D Systems) for 10 min at 95°C followed by 10 min sample cooling at room temperature, and an immediate 5 min wash in distilled water. The sample was then incubated in permeabilization solution, containing 0.5% Triton X-100+2.5% BSA in PBS three times for10 min, and then incubated with the primary antibody chicken anti-GFP at 1:50 (in 0.5% Triton X-100+2.5% BSA in PBS) for 1 h at room temperature. The sample was then washed three times for 10 min in 0.5% Triton X-100+2.5% BSA in PBS and incubated for 1 h with Alexa Fluor 488-conjugated goat anti-chicken antibody and 4′,6-diamidino-2-phenylindole (DAPI). The sample was then washed three times for 10 min each in high-salt PBS (pH 7.4) (500 mM NaCl, 20 mM Na_2HPO_4) followed by two 10 min washes in PBS. Finally, the sample was mounded in 2,2′-thiodiethanol (TDE) mounting medium (Abberior Cat. No. 4-0100-001-2) and immediately imaged under a confocal microscope (Zeiss LSM 800 with Zeiss C-Apochromat 40x/1.20 W Korr M27 and 20x PlanApochromat 20/0.8 lenses).

Western blotting and immunoprecipitation

Third instar larvae were collected and crushed in RIPA buffer [1% Triton X-100, 0.1% SDS, 0.15 M NaCl and 0.05 Tris (pH 7)] and protease inhibitors mixture (P 8340; Sigma-Aldrich), then incubated on ice for 20 min. For immunoprecipitation, equal amounts of protein lysate were incubated overnight at 4°C with protein A/G beads (SC-2003, Santa Cruz) or with GFP-TrapR_A beads (Chromotek, BioNovus Life Sciences) coupled with guinea pig anti-MSP-300 polyclonal antibody or rat anti-Ma2/d antibody, respectively. Beads were washed three times with the RIPA lysis buffer and boiled in protein sample buffer to elute the proteins. Western analysis was performed according to standard procedures, as described previously (Volk, 1992).

Statistical analysis

Distances between neighboring nuclei of muscle six were calculated using Fiji and the statistical program R, a language and environment for statistical computing (www.R-project.org). For statistics of nuclear-associated SERCA, data were acquired using a confocal microscope (Zeiss LSM 800) and analysis was performed using the profile tool (Zeiss, Zen). The average SERCA fluorescence intensity at the nuclear periphery (labeled with anti-Lamin C) relative to the nuclear interior along the nuclear meridian (Delta SERCA fluorescence) was measured. Similarly Lamin C levels at the nuclear periphery were measured relative to the nuclear exterior. Numerical analysis and statistics were performed using Excel 2013 for one-tailed *t*-test, two sample equal variance.

Microscopy and image analysis

Images were acquired at 23°C using confocal microscopes (LSM 800, Zeiss) using ZEN 2.3 system software and the following lenses: Plan-Apochromat 20×/0.8 NA M27, C-Apochromat 40×/1.20 NA W Korr M27 and Plan-Apochromat 63×/1.40 NA oil differential interference contrast (DIC) M27. Immersion media Immersol W 2010 (ne=1.3339) and Immersion oil Immersol 518 F (ne=1.518) were used.

Movies of intact larvae

To visualize dynamics of the muscle, we used a chamber developed by Ghannad-Rezaie (Ghannad-Rezaie et al., 2012). A third instar larvae expressing Ma2/d-GFP driven by Mef-GAL4 was positioned in the chamber, immobilized and placed on the stage of a VisiScope CSU-W1 Spinning Disk Confocal Microscope (Visitron Systems) attached to an Olympus IX83 inverted microscope. The images were acquired using a 60× oil immersion objective, and the acquisition duration of each image was 50 ms. Locomotion analysis was performed essentially as described by Elhanany-Tamir et al. (2012).

Acknowledgement

We thank the Bloomington Stock Center for various fly lines, the Developmental Studies Hybridoma Bank (DSHB) for antibodies and FlyBase for important genomic information. We are grateful to Mani Ramaswami and Harvey McMahon for providing

valuable primary antibodies. FlyBase is supported by a grant from the National Human Genome Research Institute at the US National Institutes of Health. The Bloomington Drosophila Stock Center is supported by a grant from the Office of the Director of the National Institutes of Health under Award Number P40OD018537.

Competing interests
The authors declare no competing or financial interests.

Author contributions
Conceptualization: A.R., T.V.; Methodology: A.R., M.S., D.L., S.W.; Investigation: A.R.; Writing - original draft: T.V.; Writing - review & editing: A.R., T.V.; Visualization: A.R., D.L.; Supervision: T.V.; Project administration: T.V.; Funding acquisition: T.V.

Funding
This study was supported by grants from the Minerva Foundation (711743 to T.V.) and the Medical Research Council (MR/N030117/1), and by the Indiana Genomics Initiative.

Supplementary information
Supplementary information available online at
http://dev.biologists.org/lookup/doi/10.1242/dev.159558.supplemental

References
Adam, J., Basnet, N. and Mizuno, N. (2015). Structural insights into the cooperative remodeling of membranes by amphiphysin/BIN1. *Sci. Rep.* **5**, 15452.
Bank, E. M., Ben-Harush, K., Wiesel-Motiuk, N., Barkan, R., Feinstein, N., Lotan, O., Medalia, O. and Gruenbaum, Y. (2011). A laminopathic mutation disrupting lamin filament assembly causes disease-like phenotypes in Caenorhabditis elegans. *Mol. Biol. Cell* **22**, 2716-2728.
Block, B. A., Imagawa, T., Campbell, K. P. and Franzini-Armstrong, C. (1988). Structural evidence for direct interaction between the molecular components of the transverse tubule/sarcoplasmic reticulum junction in skeletal muscle. *J. Cell Biol.* **107**, 2587-2600.
Cadot, B., Gache, V. and Gomes, E. R. (2015). Moving and positioning the nucleus in skeletal muscle-one step at a time. *Nucleus* **6**, 373-381.
Cain, N. E., Tapley, E. C., McDonald, K. L., Cain, B. M. and Starr, D. A. (2014). The SUN protein UNC-84 is required only in force-bearing cells to maintain nuclear envelope architecture. *J. Cell Biol.* **206**, 163-172.
Caldwell, J. L., Smith, C. E. R., Taylor, R. F., Kitmitto, A., Eisner, D. A., Dibb, K. M. and Trafford, A. W. (2014). Dependence of cardiac transverse tubules on the BAR domain protein amphiphysin II (BIN-1). *Circ. Res.* **115**, 986-996.
Canti, C., Nieto-Rostro, M., Foucault, I., Heblich, F., Wratten, J., Richards, M. W., Hendrich, J., Douglas, L., Page, K. M., Davies, A. et al. (2005). The metal-ion-dependent adhesion site in the Von Willebrand factor-A domain of alpha2delta subunits is key to trafficking voltage-gated Ca2+ channels. *Proc. Natl. Acad. Sci. USA* **102**, 11230-11235.
Cassidy, J. S., Ferron, L., Kadurin, I., Pratt, W. S. and Dolphin, A. C. (2014). Functional exofacially tagged N-type calcium channels elucidate the interaction with auxiliary alpha2delta-1 subunits. *Proc. Natl. Acad. Sci. USA* **111**, 8979-8984.
Clark, K. A., McElhinny, A. S., Beckerle, M. C. and Gregorio, C. C. (2002). Striated muscle cytoarchitecture: an intricate web of form and function. *Annu. Rev. Cell. Dev. Biol.* **18**, 637-706.
D'Alessandro, M., Hnia, K., Gache, V., Koch, C., Gavriilidis, C., Rodriguez, D., Nicot, A. S., Romero, N. B., Schwab, Y., Gomes, E. et al. (2015). Amphiphysin 2 orchestrates nucleus positioning and shape by linking the nuclear envelope to the actin and microtubule cytoskeleton. *Dev. Cell.* **35**, 186-198.
D'Arco, M., Margas, W., Cassidy, J. S. and Dolphin, A. C. (2015). The upregulation of alpha2delta-1 subunit modulates activity-dependent Ca2+ signals in sensory neurons. *J. Neurosci.* **35**, 5891-5903.
Dialynas, G., Speese, S., Budnik, V., Geyer, P. K. and Wallrath, L. L. (2010). The role of Drosophila Lamin C in muscle function and gene expression. *Development* **137**, 3067-3077.
Dialynas, G., Flannery, K. M., Zirbel, L. N., Nagy, P. L., Mathews, K. D., Moore, S. A. and Wallrath, L. L. (2012). LMNA variants cause cytoplasmic distribution of nuclear pore proteins in Drosophila and human muscle. *Hum. Mol. Genet.* **21**, 1544-1556.
Dolphin, A. C. (2012). Calcium channel auxiliary alpha2delta and beta subunits: trafficking and one step beyond. *Nat. Rev. Neurosci.* **13**, 542-555.
Dolphin, A. C. (2013). The alpha2delta subunits of voltage-gated calcium channels. *Biochim. Biophys. Acta.* **1828**, 1541-1549.
Elhanany-Tamir, H., Yu, Y. V., Shnayder, M., Jain, A., Welte, M. and Volk, T. (2012). Organelle positioning in muscles requires cooperation between two KASH proteins and microtubules. *J. Cell Biol.* **198**, 833-846.
Eroglu, C., Allen, N. J., Susman, M. W., O'Rourke, N. A., Park, C. Y., Özkan, E., Chakraborty, C., Mulinyawe, S. B., Annis, D. S., Huberman, A. D. et al. (2009). Gabapentin receptor alpha2delta-1 is a neuronal thrombospondin receptor responsible for excitatory CNS synaptogenesis. *Cell* **139**, 380-392.
Falcone, S., Roman, W., Hnia, K., Gache, V., Didier, N., Laine, J., Aurade, F., Marty, I., Nishino, I., Charlet-Berguerand, N. et al. (2014). N-WASP is required for Amphiphysin-2/BIN1-dependent nuclear positioning and triad organization in skeletal muscle and is involved in the pathophysiology of centronuclear myopathy. *EMBO Mol. Med.* **6**, 1455-1475.
Fischer, J. A., Acosta, S., Kenny, A., Cater, C., Robinson, C. and Hook, J. (2004). Drosophila klarsicht has distinct subcellular localization domains for nuclear envelope and microtubule localization in the eye. *Genetics* **168**, 1385-1393.
Folker, E. S. and Baylies, M. K. (2013). Nuclear positioning in muscle development and disease. *Front. Physiol.* **4**, 363.
Folker, E. S., Schulman, V. K. and Baylies, M. K. (2012). Muscle length and myonuclear position are independently regulated by distinct Dynein pathways. *Development* **139**, 3827-3837.
Folker, E. S., Schulman, V. K. and Baylies, M. K. (2014). Translocating myonuclei have distinct leading and lagging edges that require kinesin and dynein. *Development* **141**, 355-366.
García, K., Nabhani, T. and García, J. (2008). The calcium channel alpha2/delta1 subunit is involved in extracellular signalling. *J. Physiol.* **586**, 727-738.
Gautel, M. and Djinović-Carugo, K. (2016). The sarcomeric cytoskeleton: from molecules to motion. *J. Exp. Biol.* **219**, 135-145.
Ghannad-Rezaie, M., Wang, X., Mishra, B., Collins, C. and Chronis, N. (2012). Microfluidic chips for in vivo imaging of cellular responses to neural injury in Drosophila larvae. *PLoS ONE* **7**, e29869.
Gramates, L. S., Marygold, S. J., Santos, G. D., Urbano, J. M., Antonazzo, G., Matthews, B. B., Rey, A. J., Tabone, C. J., Crosby, M. A., Emmert, D. B. et al. and The FlyBase Consortium (2017). FlyBase at 25: looking to the future. *Nucleic Acids Res.* **45**, D663-D671.
Gundersen, G. G. and Worman, H. J. (2013). Nuclear positioning. *Cell* **152**, 1376-1389.
Hong, T. T. and Shaw, R. M. (2017). Cardiac T-tubule microanatomy and function. *Physiol. Rev.* **97**, 227-252.
Jungbluth, H. and Gautel, M. (2014). Pathogenic mechanisms in centronuclear myopathies. *Front Aging Neurosci.* **6**, 339.
Kracklauer, M. P., Banks, S. M. L., Xie, X., Wu, Y. and Fischer, J. A. (2007). Drosophila klaroid encodes a SUN domain protein required for Klarsicht localization to the nuclear envelope and nuclear migration in the eye. *Fly (Austin)* **1**, 75-85.
Lee, E., Marcucci, M., Daniell, L., Pypaert, M., Weisz, O. A., Ochoa, G. C., Farsad, K., Wenk, M. R. and De Camilli, P. (2002). Amphiphysin 2 (Bin1) and T-tubule biogenesis in muscle. *Science* **297**, 1193-1196.
Ly, C. V., Yao, C.-K., Verstreken, P., Ohyama, T. and Bellen, H. J. (2008). straightjacket is required for the synaptic stabilization of cacophony, a voltage-gated calcium channel alpha1 subunit. *J. Cell Biol.* **181**, 157-170.
Mathew, D., Popescu, A. and Budnik, V. (2003). Drosophila amphiphysin functions during synaptic Fasciclin II membrane cycling. *J. Neurosci.* **23**, 10710-10716.
Mattout, A., Pike, B. L., Towbin, B. D., Bank, E. M., Gonzalez-Sandoval, A., Stadler, M. B., Meister, P., Gruenbaum, Y. and Gasser, S. M. (2011). An EDMD mutation in C. elegans lamin blocks muscle-specific gene relocation and compromises muscle integrity. *Curr. Biol.* **21**, 1603-1614.
McGee, M. D., Rillo, R., Anderson, A. S. and Starr, D. A. (2006). UNC-83 IS a KASH protein required for nuclear migration and is recruited to the outer nuclear membrane by a physical interaction with the SUN protein UNC-84. *Mol. Biol. Cell* **17**, 1790-1801.
Metzger, T., Gache, V., Xu, M., Cadot, B., Folker, E. S., Richardson, B. E., Gomes, E. R. and Baylies, M. K. (2012). MAP and kinesin-dependent nuclear positioning is required for skeletal muscle function. *Nature* **484**, 120-124.
Mim, C. and Unger, V. M. (2012). Membrane curvature and its generation by BAR proteins. *Trends Biochem. Sci.* **37**, 526-533.
Morel, V., Lepicard, S., Rey, A. N., Parmentier, M.-L. and Schaeffer, L. (2014). Drosophila Nesprin-1 controls glutamate receptor density at neuromuscular junctions. *Cell. Mol. Life Sci.* **71**, 3363-3379.
Muchir, A. and Worman, H. J. (2007). Emery-Dreifuss muscular dystrophy. *Curr. Neurol. Neurosci. Rep.* **7**, 78-83.
Neely, G. G., Hess, A., Costigan, M., Keene, A. C., Goulas, S., Langeslag, M., Griffin, R. S., Belfer, I., Dai, F., Smith, S. B. et al. (2010). A genome-wide Drosophila screen for heat nociception identifies alpha2delta3 as an evolutionarily conserved pain gene. *Cell* **143**, 628-638.
O'Brochta, D. A., Gomez, S. P. and Handler, A. M. (1991). P element excision in Drosophila melanogaster and related drosophilids. *Mol. Gen. Genet.* **225**, 387-394.
Packard, M., Jokhi, V., Ding, B., Ruiz-Cañada, C., Ashley, J. and Budnik, V. (2015). Nucleus to synapse nesprin1 railroad tracks direct synapse maturation through RNA localization. *Neuron* **86**, 1015-1028.
Parnas, D., Haghighi, A. P., Fetter, R. D., Kim, S. W. and Goodman, C. S. (2001). Regulation of postsynaptic structure and protein localization by the Rho-type guanine nucleotide exchange factor dPix. *Neuron* **32**, 415-424.
Puckelwartz, M. and McNally, E. M. (2011). Emery-Dreifuss muscular dystrophy. *Handb. Clin. Neurol.* **101**, 155-166.

Puckelwartz, M. J., Kessler, E., Zhang, Y., Hodzic, D., Randles, K. N., Morris, G., Earley, J. U., Hadhazy, M., Holaska, J. M., Mewborn, S. K. et al. (2009). Disruption of nesprin-1 produces an Emery Dreifuss muscular dystrophy-like phenotype in mice. *Hum. Mol. Genet.* **18**, 607-620.

Razzaq, A., Robinson, I. M., McMahon, H. T., Skepper, J. N., Su, Y., Zelhof, A. C., Jackson, A. P., Gay, N. J. and O'Kane, C. J. (2001). Amphiphysin is necessary for organization of the excitation-contraction coupling machinery of muscles, but not for synaptic vesicle endocytosis in Drosophila. *Genes Dev.* **15**, 2967-2979.

Revelo, N. H. and Rizzoli, S. O. (2016). The membrane marker mCLING reveals the molecular composition of trafficking organelles. *Curr Protoc Neurosci.* **74**, 2. 25. 1-21.

Ribeiro, I., Yuan, L., Tanentzapf, G., Dowling, J. J. and Kiger, A. (2011). Phosphoinositide regulation of integrin trafficking required for muscle attachment and maintenance. *PLoS Genet.* **7**, e1001295.

Riemer, D., Stuurman, N., Berrios, M., Hunter, C., Fisher, P. A. and Weber, K. (1995). Expression of Drosophila lamin C is developmentally regulated: analogies with vertebrate A-type lamins. *J. Cell Sci.* **108**, 3189-3198.

Royer, B., Hnia, K., Gavriilidis, C., Tronchère, H., Tosch, V. and Laporte, J. (2013). The myotubularin-amphiphysin 2 complex in membrane tubulation and centronuclear myopathies. *EMBO Rep.* **14**, 907-915.

Sanyal, S., Jennings, T., Dowse, H. and Ramaswami, M. (2006). Conditional mutations in SERCA, the Sarco-endoplasmic reticulum Ca2+-ATPase, alter heart rate and rhythmicity in Drosophila. *J. Comp. Physiol. B* **176**, 253-263.

Schulman, V. K., Folker, E. S., Rosen, J. N. and Baylies, M. K. (2014). Syd/JIP3 and JNK signaling are required for myonuclear positioning and muscle function. *PLoS Genet.* **10**, e1004880.

Starr, D. A. and Han, M. (2002). Role of ANC-1 in tethering nuclei to the actin cytoskeleton. *Science* **298**, 406-409.

Subramanian, A. and Schilling, T. F. (2014). Thrombospondin-4 controls matrix assembly during development and repair of myotendinous junctions. *eLife* **3**, e02372.

Subramanian, A., Wayburn, B., Bunch, T. and Volk, T. (2007). Thrombospondin-mediated adhesion is essential for the formation of the myotendinous junction in Drosophila. *Development* **134**, 1269-1278.

Technau, M. and Roth, S. (2008). The Drosophila KASH domain proteins Msp-300 and Klarsicht and the SUN domain protein Klaroid have no essential function during oogenesis. *Fly (Austin)* **2**, 82-91.

Tian, X., Gala, U., Zhang, Y., Shang, W., Nagarkar Jaiswal, S., di Ronza, A., Jaiswal, M., Yamamoto, S., Sandoval, H., Duraine, L. et al. (2015). A voltage-gated calcium channel regulates lysosomal fusion with endosomes and autophagosomes and is required for neuronal homeostasis. *PLoS Biol.* **13**, e1002103.

Tran-Van-Minh, A. and Dolphin, A. C. (2010). The alpha2delta ligand gabapentin inhibits the Rab11-dependent recycling of the calcium channel subunit alpha2delta-2. *J. Neurosci.* **30**, 12856-12867.

Volk, T. (1992). A new member of the spectrin superfamily may participate in the formation of embryonic muscle attachments in Drosophila. *Development* **116**, 721-730.

Volk, T. (2012). Positioning nuclei within the cytoplasm of striated muscle fiber: Cooperation between microtubules and KASH proteins. *Nucleus* **4**, 18-22.

Wang, S., Reuveny, A. and Volk, T. (2015). Nesprin provides elastic properties to muscle nuclei by cooperating with spectraplakin and EB1. *J. Cell Biol.* **209**, 529-538.

Yu, X., Ma, J., Lin, F., Zhao, W., Fu, X. and Zhao, Z. J. (2012). Myotubularin family phosphatase ceMTM3 is required for muscle maintenance by preventing excessive autophagy in Caenorhabditis elegans. *BMC Cell Biol.* **13**, 28.

Zhang, Q., Bethmann, C., Worth, N. F., Davies, J. D., Wasner, C., Feuer, A., Ragnauth, C. D., Yi, Q., Mellad, J. A., Warren, D. T. et al. (2007). Nesprin-1 and -2 are involved in the pathogenesis of Emery Dreifuss muscular dystrophy and are critical for nuclear envelope integrity. *Hum. Mol. Genet.* **16**, 2816-2833.